A calibration method for realistic neutron dosimetry in radiobiological experiments assisted by MCNP simulation

Mehrdad Shahmohammadi Beni[1], Dragana Krstic[2], Dragoslav Nikezic[1,2] and Kwan Ngok Yu[1,3]*

[1]Department of Physics and Materials Science, City University of Hong Kong, Tat Chee Avenue, Kowloon Tong, Hong Kong
[2]Faculty of Science, University of Kragujevac, Serbia
[3]State Key Laboratory in Marine Pollution, City University of Hong Kong, Tat Chee Avenue, Kowloon Tong, Hong Kong
*Corresponding author. Department of Physics and Materials Science, City University of Hong Kong, Tat Chee Avenue, Kowloon Tong, Hong Kong.
Tel: +852-3442-7812; Fax: +852-3442-0538; Email: peter.yu@cityu.edu.hk
Received January 28, 2016; Revised March 23, 2016; Accepted May 9, 2016

ABSTRACT

Many studies on biological effects of neutrons involve dose responses of neutrons, which rely on accurately determined absorbed doses in the irradiated cells or living organisms. Absorbed doses are difficult to measure, and are commonly surrogated with doses measured using separate detectors. The present work describes the determination of doses absorbed in the cell layer underneath a medium column (D_A) and the doses absorbed in an ionization chamber (D_E) from neutrons through computer simulations using the MCNP-5 code, and the subsequent determination of the conversion coefficients R ($= D_A/D_E$). It was found that R in general decreased with increase in the medium thickness, which was due to elastic and inelastic scattering. For 2-MeV neutrons, conspicuous bulges in R values were observed at medium thicknesses of about 500, 1500, 2500 and 4000 µm, and these were attributed to carbon, oxygen and nitrogen nuclei, and were reflections of spikes in neutron interaction cross sections with these nuclei. For 0.1-MeV neutrons, no conspicuous bulges in R were observed (except one at ~2000 µm that was due to photon interactions), which was explained by the absence of prominent spikes in the interaction cross-sections with these nuclei for neutron energies <0.1 MeV. The ratio R could be increased by ~50% for small medium thickness if the incident neutron energy was reduced from 2 MeV to 0.1 MeV. As such, the absorbed doses in cells (D_A) would vary with the incident neutron energies, even when the absorbed doses shown on the detector were the same.

KEYWORDS: neutrons, Monte Carlo, MCNP, radiation dosimetry

INTRODUCTION

Biological effects of neutrons are relatively less studied and less well understood compared with other types of ionizing radiations such as high-energy photons and heavy ions. Neutron-induced bystander effects (NIBEs) were in general not demonstrated in early *in vitro* or *in vivo* studies [1–3]. Only recently, NIBEs were demonstrated in zebrafish embryos [4]. Similarly, results on the neutron-induced radioadaptive response (RAR) have been equivocal. Wiencke *et al.* [5] and Ng *et al.* [6] demonstrated that neutrons failed to induce a RAR in human lymphocytes and zebrafish embryos, respectively. In contrast, Marples and Shov [7] revealed a neutron-induced RAR in Chinese hamster V79 cells. Interestingly, Gajendiran *et al.* [8]

examined whole blood samples collected from 10 people, but detected a neutron-induced RAR in the samples from only one donor. Although the discrepancies between some of these results were explained in terms of mitigation of neutron-induced damages by the γ rays that were emitted together with the neutrons from the neutron sources [4, 6, 9–11], these might also have arisen because of the obscurity in the definition of the absorbed neutron dose.

Many studies on the biological effects of neutrons involve neutron dose responses, which can only be established with accurately determined absorbed doses in the irradiated cells or living organisms. Unfortunately, it is practically difficult to directly measure the absorbed doses in cells or in living organisms, and as such these are

commonly surrogated with the doses measured using some separate radiation detectors such as an ionization chamber. However, it might not be straightforward to ascertain the 'conversion coefficients' between the neutron doses (D_E) recorded by such radiation detectors placed in the ambient environment and the neutron doses (D_A) actually absorbed in the exposed cells or living organisms, since both D_E and D_A critically depend on the dimensions, geometries and densities of these various exposed targets, the materials surrounding the exposed targets, and the energy of the incident neutrons. The present study used *in vitro* experiments with cells as an example to demonstrate how the conversion coefficients R ($= D_A/D_E$) could be determined through computer simulation using the MCNP (Monte Carlo N-Particle) code [12].

In fact, the task was similar to the development of concepts in the field of radiation protection. Traditionally, for radiation protection purposes, three categories of 'quantities' have been defined, namely (i) 'physical quantities' such as air kerma for photons and absorbed dose for β particles; (ii) 'protection quantities' (or 'primary limiting dose quantities') such as organ absorbed dose, organ equivalent dose, and effective dose; and (iii) 'operational quantities' such as the ambient dose equivalent $H^*(d)$, the directional dose equivalent $H'(d,\Omega)$ and the personal dose equivalent $H_p(d)$ [13] defined using the ICRU sphere phantom with a diameter of 30 cm built with a tissue-equivalent material (density = 1 g cm^{-3}; mass composition: 76.2% oxygen, 11.1% carbon, 10.1% hydrogen and 2.6% nitrogen). While the protection quantities were defined to characterize the risk of exposures to ionizing radiations, these were in general not measurable. As such, operational quantities were required that characterized the external exposures, either to an area or to an individual. Operational quantities could be calculated from physical quantities using the ICRU sphere phantom, while protection quantities could also be calculated from physical quantities using anthropomorphic phantoms together with the radiation weighting factors W_R and the tissue weighting factors W_T. As such, measurements on operational quantities could provide information

on the protection quantities. The conversion coefficients for these quantities have been published by ICRP [14, 15].

The similarities between the task in the present work and the development of concepts in the field of radiation protection are summarized in Fig. 1. Both the absorbed dose in the cells (D_A) and the protection quantities described above gave directly relevant information in that they were used to establish realistic dose responses and to characterize the risk of exposures to ionizing radiations. However, both were practically difficult to measure. The role of the neutron doses (D_E) specified for neutron irradiation obtained from a detector in the present work was similar to the role of the operational quantities described above, with the former providing information on the absorbed dose in the cells and the latter providing information on the protection quantities. While operational and protection quantities could be calculated from physical quantities as described above, the neutron doses (D_E) absorbed in the detector and the absorbed dose (D_A) absorbed in the cells could be calculated using the MCNP-5 code from information on the dimensions of the detector and the cell layer, respectively. The conversion coefficients R ($= D_A/D_E$) then played a similar role as the conversion coefficients between the protection and operational quantities.

The present work examined the dependence of R on the thickness of the medium above the cell layer, the thickness of the cell layer itself, and the energy of neutrons. It was not our intention to give exhaustive results for all possible combinations of these parameters. Instead, the present work focused on outlining the concept and on proposing the methodology for determining the R values. The concept and methodology can be easily extended to studies with different detectors (e.g. with different dimensions and/or materials), different targets (e.g. targets with different geometries, and targets underneath medium of different thicknesses), neutrons with different energies or with different energy spectra, or even different types of ionizing radiations. Once the conversion coefficient R can be accurately determined for an experimental set-up, the doses absorbed by the irradiated cells or living organisms can be
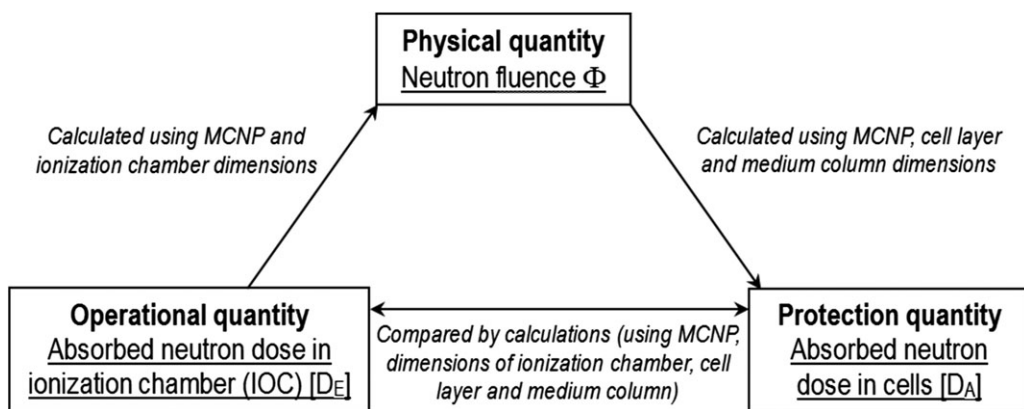

Fig. 1. Comparison between the task in the present work and the development of concepts in the field of radiation protection. The quantities in bold are those in the field of radiation protection (i.e. operational quantity, physical quantity and protection quantity). The underlined quantities are those considered in the present work (i.e. absorbed neutron dose in ionization chamber (IOC), neutron fluence (Φ) and absorbed neutron dose in cells). The task in the present work was to obtain the conversion coefficient R ($= D_A/D_E$), with the procedures shown in the italicized descriptions.

realistically determined to provide accurate information on the dose responses.

MATERIALS AND METHODS

In the present work, in order to demonstrate the concept of and methodology for deriving the conversion coefficient R, references were made to the realistic conditions at the Neutron Exposure Accelerator System for Biological Effects Experiments (NASBEE) at National Institute of Radiological Sciences (NIRS), Chiba, Japan, where details regarding the neutron energy, irradiation set-up and the detector for quantifying the neutron dose were fully available. The quasi-monoenergetic neutrons in the NASBEE facility were generated by the Be(d–n)B reaction and had an average energy of 2 MeV. The neutron doses specified for neutron irradiation were obtained from an ionization chamber (IOC) (IC-17A, Far West Technology) [16]. Furthermore, the contamination of γ-rays was measured at a source-to-target distance (STD) of 1170 mm using an LET counter (F.W.T. LET-1/2, Far West Technology) and was found to be 14% [16].

The task was to determine the relationship between D_A and D_E, and the procedures are shown in Fig. 1. The neutron source was modeled as a circular mono-directional disk source. The diameter of the irradiation field was defined by the radius of this source. In principle, the neutron fluence Φ was the physical quantity that controlled both D_A and D_E. As such, once we knew D_E, Φ could be determined to give D_A. By referring to the dimensions and materials of the ionization chamber, the neutron fluence Φ could be determined through iterations to reproduce D_E through MCNP simulations. From the determined Φ value, and by referring to the dimensions and materials of the cell layer and the culture-medium column, D_A could also be computed through MCNP simulations. In the present paper, contributions from neutrons and the generated photons were taken into account. The absorbed dose was quantified as the energy deposition in each domain (in MeV/g) determined using the track length estimate of the energy deposition (tally F6:NP). In fact, the MCNP-5 code could give the dose deposited per unit neutron, so we could directly focus on the conversion coefficients R, defined as the ratio (D_A/D_E) if explicit evaluation of Φ was not necessary.

Absorbed neutron dose D_E in an ionization chamber

The IOC described above had a volume of 1 ml, with 0.127 cm thickness of tissue-equivalent plastic (TEP) (density = 1.127 g/cm^3) and an outer diameter of 15 mm, and it was filled with air (see the schematic diagrams in Fig. 2). The characteristics of the IOC are summarized in Table 1. In realistic situations, the IOC was calibrated using a ^{60}Co γ-ray source [16]. The dose delivered per incident neutron in the air volume enclosed by TEP was computed using MCNP-5.

Absorbed neutron dose D_A in cells

Suda *et al.* [16] used T25 cell culturing flasks (Falcon) with a surface area of 25 cm^2 to hold the cells (contained in 3 ml of cell-culture media) for irradiation. Accordingly, in our model, the flask was modeled as a cylinder with a surface area of 25 cm^2. The surface area was an important parameter because it controlled the susceptibility of target volumes during neutron irradiation.

A variety of cell and medium thicknesses (and thus volumes) were investigated. The cell thicknesses were measured from the bottom of the cylindrical flask, and those cells were assumed to be at 100% confluence. The materials of the cells and culture medium were surrogated with TEP and water, respectively. Tables 2 and 3 summarize the cell thicknesses (between 10 and 30 μm) and medium thicknesses (between 100 and 5000 μm) considered in the present work. The cell irradiation set-up for neutron exposure is schematically shown in Fig. 3. The cells were located at the bottom of the medium, so the neutrons needed to pass through the liquid medium before they could interact with the cells. Air was considered to be surrounding the medium column and the cell layer, as was the case in the real-life experimental set-up. The distance between the neutron source and the cell layer (target), referred to as the STD, was fixed at 710 mm [16]. When the medium thickness was increased, the distance between medium surface and source would decrease.

In this work, the neutron transport mode in MCNP-5 was used to determine the energy deposited in the cell layer per incident neutron. In order to achieve good statistical power, a total of 10^4
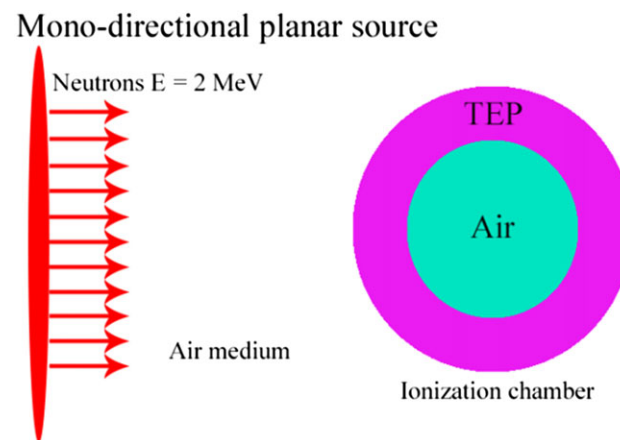

Fig. 2. Schematic diagram showing the set-ups for neutron irradiation for determining the dose per neutron deposited in the ionization chamber IC-17A (1 ml chamber enclosed by a 0.127 cm thick wall of tissue-equivalent plastic [TEP]).

Table 1. Summary of geometry and dimensions of the ionization chamber (IOC) with a tissue equivalent plastic (TEP) wall

Geometry	Outer diameter	Inner diameter	Thickness of TEP	Volume
Spherical	1.5 cm	1.246 cm	0.127 cm	1 ml

Table 2. Thicknesses and volumes of cell layers considered in the present work

No.	Thickness (μm)	Volume (ml)
1	10	0.025
2	15	0.037
3	20	0.050
4	25	0.062
5	30	0.075

Table 3. Thicknesses and volumes of the medium columns above the studied cell layers considered in the present work

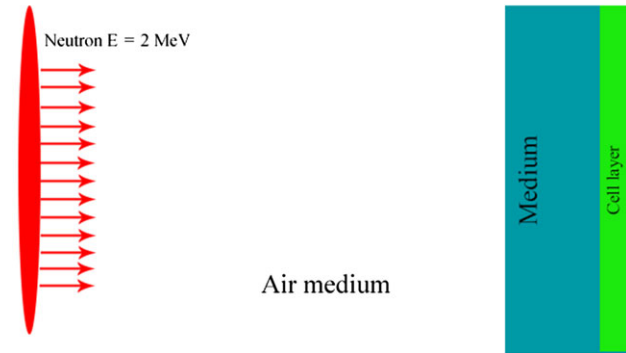| No.	Medium thickness (μm)	Medium volume (ml)
1	100	0.25
2	500	1.25
3	1000	2.50
4	1500	3.75
5	2000	5.00
6	2500	6.25
7	3000	7.50
8	3500	8.75
9	4000	10.00
10	4500	11.25
11	5000	12.50

Fig. 3. Schematic diagram showing the neutron irradiation set-up for determining the dose per neutron deposited in the cell layer covered by medium of various thicknesses.
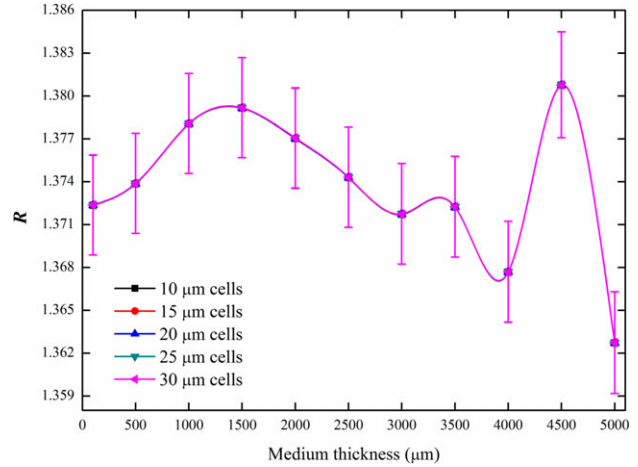

Fig. 4. Ratios R between dose absorbed in the cell layer and dose absorbed in the ionization chamber from 2-MeV neutrons with varying medium thicknesses. The uncertainties were computed from the relative errors provided in the outputs from the MCNP simulations.

neutrons were employed for each calculation. The relative errors for the energy deposition tally were ~3–4%.

RESULTS AND DISCUSSIONS

By using MCNP-5, the dose D_E deposited in an IOC per 2-MeV neutron was determined as 6.50×10^{-15} Gy. Figure 4 shows the ratios R $(= D_A/D_E)$ for 2-MeV neutrons for varying medium thicknesses. It can be observed that the thickness of the medium has a major effect on the absorbed dose in the cell layer. In general, R decreases with increase in the medium thickness. This is expected since it is more likely that the neutrons emitted from the source will interact with the medium when its thickness increases. In hydrogenous media such as water, the neutron speed will be reduced due to elastic and inelastic scattering with light nuclei (hydrogen nuclei). In our case, the energy of the neutrons was fixed at 2 MeV, and these 'fast' neutrons mainly lost their energies through elastic collisions. The trends were not significantly different for different cell-layer thicknesses (between 10 and 30 μm), which was expected since neutron collisions and thus neutron energy deposition mainly

occurred in the medium above the cell layer due to the much larger thickness of the medium compared with the thickness of the cell layer. In Fig. 5, the dose per incident neutron delivered to the water medium above a cell layer of varying thickness is shown, which demonstrates that the dose in general increases with the medium thickness. In other words, neutrons can deposit more energy in medium with larger numbers of nuclei. However, the energy deposition and its pattern are also highly dependent on the interaction cross sections between the neutrons and the nuclei.

Conspicuous bulges in the R values are observed at different medium thicknesses, such as about 1500, 3500 and 4500 μm, and these are attributed to the presence of carbon, nitrogen and oxygen nuclei in the medium, and are reflections of the spikes in the
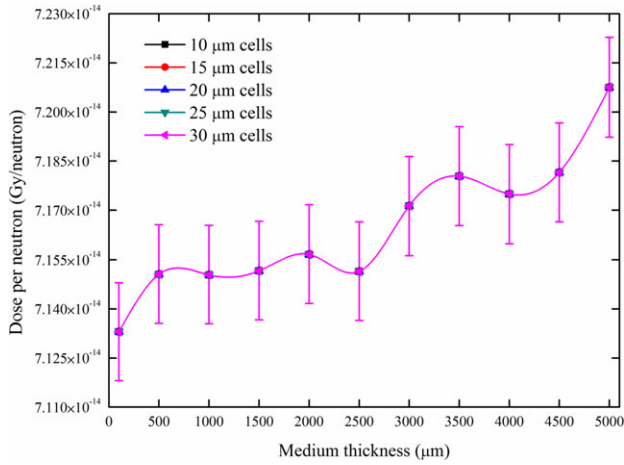
Fig. 5. Dose per incident 2-MeV neutron delivered to the water medium above a cell layer of varying thickness. The uncertainties were computed from the relative errors provided in the outputs from the MCNP simulations.

neutron interaction cross sections for these nuclei shown in Fig. 6 (from Evaluated Nuclear Data File [ENDF/B-VI]). When the neutrons interacted with nuclei within the medium, their energies were reduced and could fall into cross-section regimes containing the spikes.

Furthermore, the dependence of R on the medium thickness was determined for incident neutrons with an energy of 0.1 MeV. By using MCNP-5, the dose D_E deposited in an IOC per 0.1-MeV neutron was determined to be 7.52×10^{-16} Gy. No conspicuous bulges were found in the R values for medium thicknesses of between 0 and 5000 μm (except for one at ~2000 μm, which was due to photon interactions), and this was explained by the absence of prominent spikes in the interaction cross sections with carbon, oxygen and nitrogen nuclei for neutron energies <0.1 MeV (see Fig. 6a to d). Considering the significantly different interaction cross sections with hydrogen, carbon, oxygen and nitrogen nuclei for neutrons with different energies, it was interesting to examine the ratio R for 0.1-MeV neutrons, the results of which are shown in Fig. 7. By comparing the results in Figs 4 and 7, R could be increased by ~50% for small medium thicknesses if the incident neutron energy
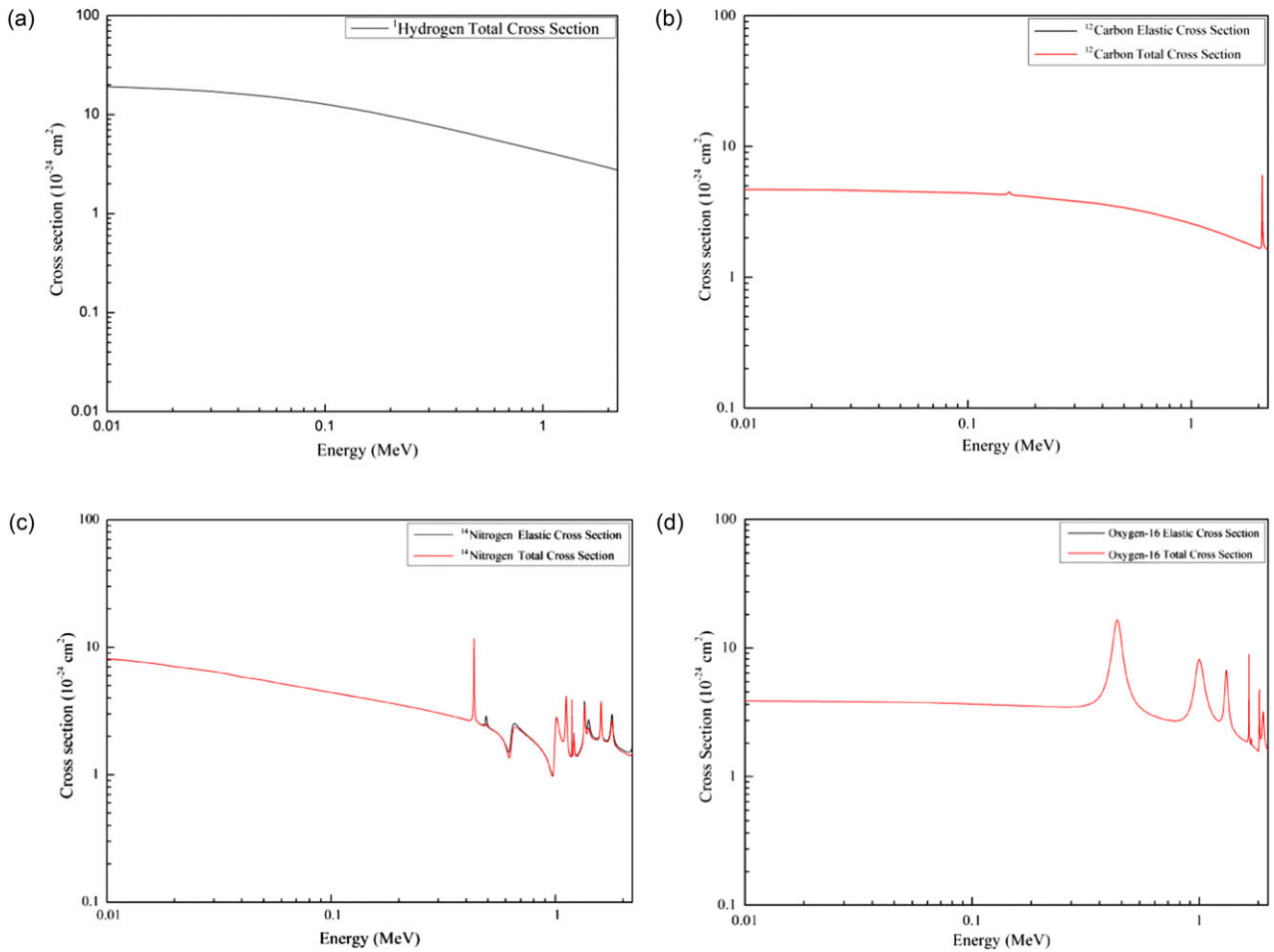

Fig. 6. Neutron interaction cross sections for (a) hydrogen, (b) carbon, (c) nitrogen and (d) oxygen nuclei.
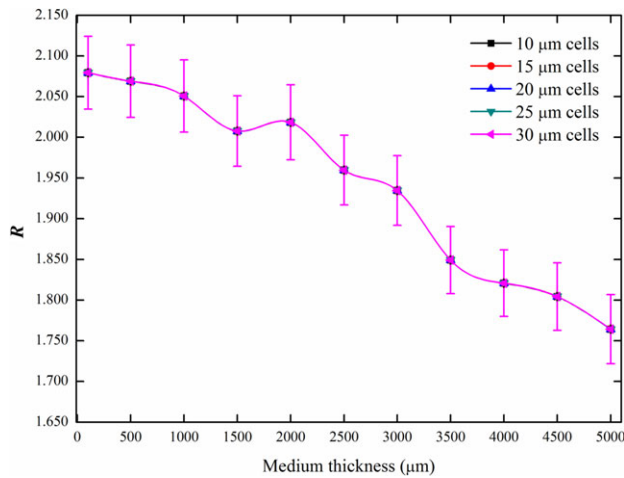
Fig. 7. Ratios *R* between dose absorbed in the cell layer and dose absorbed in the ionization chamber from 0.1-MeV neutrons for varying medium thicknesses. The uncertainties were computed from the relative errors provided in the outputs from the MCNP simulations.

was reduced from 2 MeV down to 0.1 MeV. As such, it was pertinent to note that the absorbed doses in cells (D_A) would vary with the incident neutron energies, even when the absorbed doses shown on the detector were the same.

CONCLUSIONS

The present work outlined the concept of and proposed methodology for determining the ratios *R* between the doses absorbed in the cell layer underneath a medium column (D_A) and the dose absorbed in an IOC (D_E) from neutrons. The realistic values of D_A and D_E were determined through computer simulations using the MCNP-5 code. The ratios *R* in general decreased with the medium thickness, and this was due to elastic and inelastic scattering. For 2-MeV neutrons, conspicuous bulges in the *R* values were observed at medium thicknesses of about 1500, 3500 and 4500 μm, and these were attributed to the presence of carbon, oxygen and nitrogen nuclei, and were reflections of the spikes in their interaction cross sections with neutrons. For 0.1-MeV neutrons, no conspicuous bulges in the *R* values were observed (except for one at ~2000 μm, which was due to photon interactions), and this was explained by the absence of prominent spikes in the interaction cross sections with carbon, oxygen and nitrogen nuclei for neutron energies <0.1 MeV. The ratios *R* could be increased by ~50% for small medium thickness if the incident neutron energy was reduced from 2 MeV down to 0.1 MeV. Therefore, the absorbed doses in cells (D_A) would vary with the incident neutron energies, even when the absorbed doses shown on the detector were the same. The above results have far-reaching implications for realistic establishment of dose–response relationships for studies on the radiobiological effects of neutrons. The concept and methodology can also easily be extended to studies with different detectors, different targets, neutrons with different energies or with different energy spectra, or even different types of ionizing radiations.

CONFLICT OF INTEREST

The authors declare that there are no conflicts of interest.

REFERENCES

1. Liu Z, Mothersill CE, McNeill FE, et al. A dose threshold for a medium transfer bystander effect for a human skin cell line. *Radiat Res* 2006;166:19–23.
2. Seth I, Schwartz JL, Stewart RD, et al. Neutron exposures in human cells: bystander effect and relative biological effectiveness. *PLoS One* 2014;9:e98947.
3. Wang C, Smith RW, Duhig J, et al. Neutrons do not produce a bystander effect in zebrafish irradiated *in vivo*. *Int J Radiat Biol* 2011;87:964–73.
4. Ng CYP, Kong EY, Kobayashi A, et al. Neutron induced bystander effect among zebrafish embryos. *Radiat Phys Chem* 2015;117:153–9.
5. Wiencke JK, Shadley JD, Kelsey KT, et al. Failure of high intensity x-ray treatments or densely ionizing fast neutrons to induce the adaptive response in human lymphocytes. In: Fielden EM, Fowler JF, Hendry JH, Scott D (eds). *Radiation Research*. Vol. 1. London: Taylor and Francis, 1987, 212.
6. Ng CYP, Kong EY, Kobayashi A, et al. Non-induction of radioadaptive response in zebrafish embryos by neutrons. *J Radiat Res* 2016. 10.1093/jrr/rrv089.
7. Marples B, Skov KA. Small doses of high-linear energy transfer radiation increase the radioresistance of Chinese hamster V79 cells to subsequent X irradiation. *Radiat Res* 1996;146:382–7.
8. Gajendiran N, Tanaka K, Kumaravel TS, et al. Neutron-induced adaptive response studied in G0 human lymphocytes using the comet assay. *J Radiat Res* 2001;42:9l–101.
9. Scott BR, Di Palma J. Sparsely ionizing diagnostic and natural background radiation are likely preventing cancer and other genomic-instability associated diseases. *Dose Response* 2006;5:230–55.
10. Portess DI, Bauer G, Hill MA, et al. Low-dose irradiation of nontransformed cells stimulates the selective removal of precancerous cells via intercellular induction of apoptosis. *Cancer Res* 2007;67:1246–53.

11. Ng CYP, Kong EY, Konishi T, et al. Low-dose neutron dose response of zebrafish embryos obtained from the Neutron exposure Accelerator System for Biological Effect Experiments (NASBEE) facility. *Radiat Phys Chem* 2015;114:12–7.

12. X-5 Monte Carlo Team. *MCNP–a General Monte Carlo N-Particle Transport Code, Version 5. Vol. I: Overview and Theory.* Los Alamos: Los Alamos National Laboratory. LA-UR-03-1987, 2003.

13. ICRU. Radiation quantities and units. *ICRU Report 33.* Washington: ICRU, 1980.

14. ICRP. Conversion coefficients for use in radiological protection against external radiation. ICRP Publication 74, *Annals of ICRP* **26** (3–4), 1996.

15. ICRP. Conversion coefficients for radiological protection quantities for external radiation exposures. ICRP Publication 116, *Annals of ICRP* **40** (2–5), 2010.

16. Suda M, Hagihara T, Suya N, et al. Specifications of a neutron exposure accelerator system for biological effects experiments (NASBEE) in NIRS. *Radiat Phys Chem* 2009;78:1216–9.